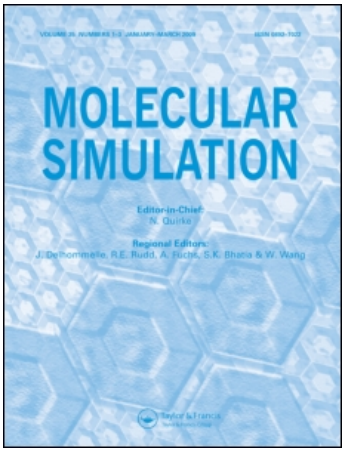

Molecular Simulation
Publication details, including instructions for authors and subscription information:
http://www.informaworld.com/smpp/title~content=t713644482

Molecular Dynamics of Coat Proteins of the Human Rhinovirus

Wan F. Lau[a]; B. Montgomery Pettitt[a]; Terry P. Lybrand[ab]
[a] Department of Chemistry, University of Houston, Houston, Texas, USA [b] Department of Medicinal Chemistry and Pharmacognosy, University of Minnesota, Minneapolis, Minnesota, USA

To cite this Article Lau, Wan F. , Pettitt, B. Montgomery and Lybrand, Terry P.(1988) 'Molecular Dynamics of Coat Proteins of the Human Rhinovirus', Molecular Simulation, 1: 6, 385 — 398
To link to this Article: DOI: 10.1080/08927028808080960
URL: http://dx.doi.org/10.1080/08927028808080960

Molecular Simulation, 1988, Vol. 1, pp. 385–398
Reprints available directly from the publisher
Photocopying permitted by license only

MOLECULAR DYNAMICS OF COAT PROTEINS OF THE HUMAN RHINOVIRUS

WAN F. LAU, B. MONTGOMERY PETTITT* and TERRY P. LYBRAND†

Department of Chemistry, University of Houston, Houston, Texas 77204-5641, USA

(*Received April 1988; in final form July, 1988*)

The effects of the oxazole antiviral WIN 52084 on the thermal vibrations of the coat proteins of the human rhinovirus were studied by means of a comparison of two molecular dynamics simulations. One simulation involved only a protomeric unit (cluster of four proteins) of the viral coat, while the other included the antiviral drug bound to the protein cluster. Analysis of the RMS fluctations for all atoms indicates that the drug did not cause any statistically significant global changes in the amplitude of atomic motion. However, the RMS fluctuation of seventeen residues in the vicinity of the drug decreased by about 11%. Two global effects were observed. Most importantly, the drug was found to make the decay times of the atomic fluctuations more uniform. Also, the drug lowered the average correlation time for displacements of atoms in the drug-bound cluster. Finally, a comparison of the differences in the normalized cross-correlation functions of residues close to the binding site showed that the residues move more collectively and in phase in the presence of the ligand. These results indicate that the drug has a global effect on the dynamics of the protein cluster and suggest a simple mechanical model for the action of the drug.

KEY WORDS: coat proteins, human rhinovirus, thermal vibrations, molecular dynamics.

INTRODUCTION

Molecular dynamics calculations have been used to study the types of motion that occur in a number of proteins and nucleic acids during time intervals of ten to a few hundred psec (1). These include simulations that do not explicitly include the solvent surroundings, for example bovine pancreatic trypsin inhibitor (BPTI) (2), phenylalanine transfer RNA (3), and ferrocytochrome c (4), as well as simulations in an aqueous environment, for example, BPTI and avian pancreatic polypeptide hormone (APP) in hydrated crystals (5), trypsin in water (6), and parvalbumin (7). Molecular dynamics has also been used to study the dynamics of protein-substrate complexes, for example, trypsin (6), parvalbumin (7), ribonuclease (8) and lysozyme (9).

Recently, the availability of crystal structures of a picornavirus, the human rhinovirus HRV14 (10) with and without antivirals bound to the protein coat has made it possible to study the dynamics of this complex system. Picornaviruses comprise one of the largest families of viral pathogens and cause numerous diseases in humans and animals (11). Besides the rhino (common cold) viruses, they also include the polioviruses, cardioviruses and foot-and-mouth viruses, and a host of other agents of disease. A thermodynamic simulation technique (12), is being used in a separate

†Present Address: *Department of Medicinal Chemistry and Pharmacognosy, University of Minnesota, Minneapolis, Minnesota 55455, USA*

project to study the thermodynamics of solvation and binding of the antivirals to the coat protein (13).

We report here a parallel study on the dynamics of the drug-free and drug-bound proteins. This is an initial effort toward understanding the effect of the antiviral, WINJ 52084, (Figure 1) on the dynamics and activity of HRV14. The drug is an analog of the oxazole family of antivirals which have been shown to have a broad spectrum of activity against picornaviruses (14). Such information could help in the design of new antivirals for HRV14, and perhaps also for other picornaviruses. In addition, simulations of the dynamics of the coat proteins could provide some insight into the process of virion assembly and into the uncoating process that precedes viral replication (10, 14).

For this exploratory study, the simplest structural unit, a cluster of four distinct polypeptides called the protomeric unit, was chosen for the simulations (see discussion). One simulation involved the drug-free (apoprotein) cluster, while the other involved the drug-bound (holoprotein) cluster. An analysis is made of the effects of the drug on the thermal vibrations of the coat proteins of the human rhinovirus by comparison of the 10 psec trajectories from the two simulations.

METHODS

We used the crystal structure of the holoprotein (drug-bound), kindly provided by Michael Rossmann and co-workers (10) for the starting coordinates of both of the simulations. For the simulation of the apoprotein, the coordinates of the ligand were removed from the crystal structure file. Although a crystal structure for the apoprotein exists, we chose to use the holoprotein structure as the source for the apoprotein structure in order to facilitate comparison of the differences in the simulations (e.g., the effects of the drug on the thermal vibrations of the protein), it being less likely that any differences obtained are the results of different starting structures. While this prevents artifacts from the use of different starting crystal coordinates, it provides another source of ambiguity in the final analysis, which we will return to later in the discussion. In the present study we shall refer to this as the reference crystal structure for the drug free protomer.

The forces on the atoms and their dynamics were calculated with the CHARMM program. The methodology and the general form of the potential functions were as previously described elsewhere (15). No explicit hydrogen bond potential was used; instead, it is assumed to be adequately accounted for by the Coulomb and Lennard-Jones terms. In both the minimizations and dynamics, the non-bonded interactions were calculated using a constant dielectric of 1.0, with a cutoff distance of 8.5 Å. An interaction switching function with an "on" distance of 7.0 Å and an "off" distance of 8.0 Å was used. Polar hydrogen atoms were explicitly included in the simulations.

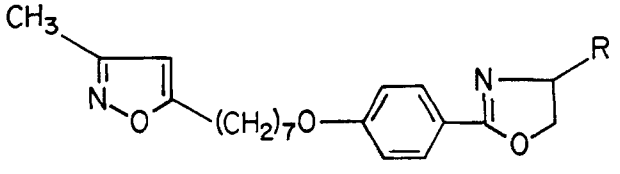

Figure 1 Schematic structure of drug molecules WIN 51711 (R = H) and WIN 52084 (R = methyl).

There were 7639 atoms (or 804 residues) in the apoprotein and 7665 atoms in the holoprotein structures. The X-ray crystal structures were refined by executing 100 steps of steepest descent (SD) minimization, followed by 100 steps of Adopted Basis Newton-Raphson (ABNR) minimization (15). For the dynamics, the Verlet algorithm was used (16) and SHAKE (17) was applied to the hydrogens. Using a timestep of 0.001 psec, the non-bonded list was updated every 10 steps, and coordinates and statistics were collected every 10 steps. The minimized protein structures were each heated slowly from 100 to 300 K in 10° increments every 200 steps over a period of 4 psecs. The proteins were then equilibrated at 300 K for 2 psecs, with velocity scaling every 200 steps. The apoprotein and holoprotein were equilibrated without intervention for a further 8 psecs and 7 psecs, respectively. After equilibration, 10 psec trajectories were collected for each of them. The simulations were performed in a microcanonical ensemble (N, V, E) without any velocity scaling. The average temperatures at the beginning of the trajectories, as measured by the kinetic energy of the protein, were 302 K for the apoprotein and 299 K for the holoprotein. The drift in total energy over the course of 10 psecs was 4 kcal/mol (0.08%) for the apoprotein and 12 kcal/mol (0.17%) for the holoprotein. The ratio of the RMS fluctuations in the total energy to those in the kinetic energy was less than 0.02, an acceptable value for integrator stability (15, 17).

From each trajectory, 1000 coordinate sets at 0.01 psec intervals were collected and used to analyze the atomic fluctuations, including the normalized auto-correlation and cross-correlation functions of the displacement vectors for the C_α atoms of residues in the vicinity of the drug binding site. The normalized correlation $C_a(t)$ for a dynamical variable $A(t)$ is calculated by means of the expression,

$$C_a(t_n) = \frac{\sum_{m=1}^{N-n} A(t_m) \cdot A(t_m + t_n)}{\frac{N-n}{N} \sum_{m=1}^{N} [A(t_m)]^2} \quad (1)$$

where $A(t_m)$ is the value of the variable at t_m ($m = 1,2, \ldots N$).

In addition, the time correlation functions for the atomic displacements of every fifth residue of the clusters were calculated. Certain regions were selected for closer examination (see Results and Discussion) and the correlation functions of every residue in such regions were calculated. We restricted our analysis of the above correlation functions to those of the C_α atoms only. For simplicity, we estimated the relaxation time τ by a least squares fit of the correlation time to the expression

$$C(t) = A \exp(-t/\tau) \quad (2)$$

Dynamically averaged structures of the clusters at 5 psec and 10 psec were obtained from the trajectories. These and the energy minimized structures were compared to the corresponding X-ray crystal structures.

The R factor for each structure was taken to be

$$R = \left[\sum_{i=1}^{N} m_i |r_{i,a} - r_{i,x}|^2 \Big/ \sum_{i=1}^{N} m_i \right]^{0.5} \quad (3)$$

The quantity m_i is the mass of atom i, and $r_{i,a}$ and $r_{i,x}$ are its coordinates in the average conformation and in the X-ray structure, respectively.

Finally, the radius of gyration, r_g was calculated from the expression

$$r_g^2 = \frac{\Sigma\, m_i r_i^2}{\Sigma m_i} \tag{4}$$

where m_i is the mass of atom i and r_i is its distance from the center of mass of the protein.

RESULTS AND DISCUSSION

1. General Structure of the Proteins

To facilitate the discussion of the dynamic results and their relation to the structural features of the viral coat proteins, we include here a brief overview of the structure and organization of the proteins (Figures 2a, b). The spatial relationships of VP1, VP2 and VP3 are indicated in Figure 2a. VP4 is an extended polypeptide chain that is positioned internally below the three subunits (18). Both the amino and carboxyl ends of VP1 and VP3 are intertwined with each other. VP2 is globular and does not intertwine with the other two proteins extensively. However, it is in contact with these proteins via VP4 which contacts VP1 and VP2. Hence, the dynamics of one subunit could influence the dynamics of the other subunits via these contacts. As seen in Figure 2, the amino and carboxyl ends of VP1 and VP3 make excursions outside of the triangular cluster. These ends clearly play a role in the association of the triangular unit with proteins of adjacent units.

The triangular unit shown in Figure 2 is the crystallographic unit. The pentagonal unit made up of five such clusters dissociates in solution into five somewhat different units. The latter, termed sedimentary units, consist of VP1, VP2 and VP4 of one

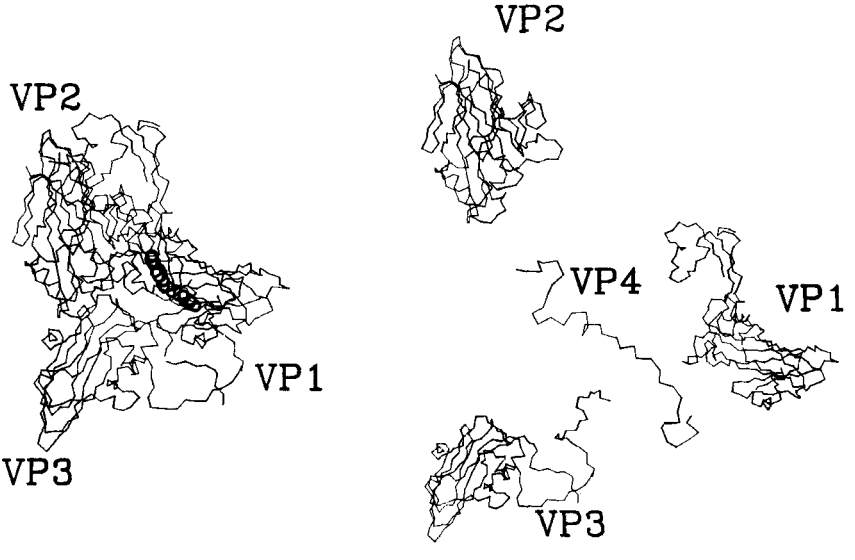

Figure 2a C_α atom drawing of the crystallographic unit of a viral protein, with bound ligand (Van der Waals radii for the ligand). **2b** Drawing of individual subunits of the crystallographic unit, showing their relative positions within the unit.

crystallographic unit and VP3 from the adjacent unit on its right (see Figure 2). As we were interested in studying the effects of the drug on functional as well as physical aspects of the protein coat, the crystallographic unit was chosen because it contains a boundary plane of separation of the sedimentary units. The drug binds with a central location near the corner of the 5-fold axis, close to the boundary of separation.

The effects of minimization and dynamics on the protein structure are presented in Table I, which gives the RMS difference of the structures of the clusters (free and bound) at different stages, compared to the corresponding starting crystal structure. After 200 steps of minimization (100 SD, 100 ABNR) to relieve stress in the crystal structure, the RMS difference was only 0.58 Å (C_α only; 0.73 Å for all atoms) for both complexes. The RMS difference over all atoms for the 10 psec dynamics averaged structures was 2.62 Å and 2.49 Å for the free and bound complexes, respectively. The various contributions to the RMS difference from each segment are also given in Table I. VP1 and VP3 had relatively large differences in both complexes, but this is primarily due to the carboxyl ends and a loop in VP3 (see Figure 2). The atoms in these segments can move around more or less freely, and these segments are considerably displaced from the crystal structure. If the free amino and carboxyl ends of VP1 of the drug-free cluster are excluded, the RMS difference is only 1.25 Å. This is similar to the value for VP2, which does not have these free excursions at the surface of the cluster. Although VP4 is a relatively linear strand with little secondary structure (i.e., stable β-sheets or helices), it has a rather low RMS difference. This is likely due to its proximity to portions of VP1 and VP2, which act to stabilize it. The RMS deviations for the C_α atoms of VP2 and VP4 are close to that reported in other simulations, 1.5 Å for lysozyme (9), BPTI (19) and ferrocytochrome c (4, 20).

It can be seen from Table I that the presence of the drug affected the dynamics of the various segments differently. Although the RMS differences for each segment were similar for the two clusters at the start of the simulation, they were less similar in the 10 psec dynamics averaged structure. VP1 and VP4 had smaller RMS differences

Table I Mass Weighted RMS Deviation of Drug-Free Cluster from Reference Crystal Structure[a]

	100 steps SD[b]	*100 steps ABNR*[c]	*5 psec.*	*10 psecs.*
Whole Cluster	0.306 (0.406)	0.584 (0.732)	2.637 (2.904)	2.623 (2.892)
VP1	0.309	0.576	1.882	2.997
VP2	0.297	0.576	1.179	1.200
VP3	0.279	0.575	2.017	3.043
VP4	0.285	0.634	1.292	1.402

Mass Weighted RMS Deviation of Drug-Bound Cluster from Crystal Structure[a]

	100 steps SD[b]	*100 steps ABNR*[c]	*5 psec.*	*10 psec.*
Whole Cluster	0.303 (0.404)	0.585 (0.733)	2.535 (2.734)	2.491 (2.696)
VP1	0.306	0.574	2.403	2.364
VP2	0.321	0.573	1.114	1.913
VP3	0.276	0.579	3.467	3.393
VP4	0.282	0.652	1.211	1.162

[a] R-factors for C_α carbons only. Values in brackets reflect all atoms. All values are in Å.
[b] Steepest descent energy minimization.
[c] Adopted Basis Newton-Raphson energy minimization.

while VP2 and VP3 had greater differences in the bound cluster compared to the free cluster.

The original crystal structures of the drug-free and drug-bound clusters are very similar, differing only in the chain leading from the FMDV loop of VP1 across the "canyon" floor (res 213 to 225), and in residues at the carboxyl end of the βE corner of VP1 (res 150 to 157) (10). In the crystal structures, the RMS differences were 0.660 Å for VP1, 1.825 Å for res 213 to 225, and 0.477 Å for res 150 to 157. The corresponding RMS differences between the 10 ps dynamic averaged drug-free structure and the X-ray structures were 2.997 Å, 0.687 Å, and 1.082 Å for the drug-bound X-ray structure, and 3.061 Å, 1.771 Å, and 0.961 Å for the drug-free X-ray structure. These results suggest that, during the 10 ps period of dynamics with no drug bound, the cluster had not moved much from the drug-bound conformation toward the drug-free conformation.

The RMS difference between the 10 psec dynamics structure of the bound versus the free proteins was 2.153 Å for the entire protomer, 2.424 Å for VP1, 0.958 Å for VP2, 2.377 Å for VP3 and 1.129 Å for VP4. These values are smaller than those of the RMS differences with the crystal structure (Table I). However, given that the starting crystal structures were the same except for the presence of the drug, the two simulations clearly led to different structures. The RMS difference for C_α atoms within 20 Å of the drug was only 0.997 Å. This smaller difference reflects the absence of contributions from the highly variable loops and terminal ends.

Similarly, the RMS differences for C_α atoms within 20 Å of the drug site in the drug-free dynamics versus crystal structures were 1.502 Å for dynamics vs. original crystal structure and 1.214 Å for dynamics versus reference crystal structure used for the simulations, while the difference between the drug-bound dynamics versus drug-bound crystal structure was smaller for the case of the drug-bound protein cluster (1.066). Hence, the ligand appears to reduce the RMS difference.

An analysis was performed on the changes in the water accessible surface area (21) of the protein clusters, with the results given in Table II. The overall percentage decrease in the surface area of the 10 psec averaged structures was similar for both

Table 2 Changes in Water Accessible Surface Area for Drug-Free Cluster

	Crystal[a]	*100 steps S.D.*[b]	*100 steps ABNR*[b]	*5 psec.*[b]	*10 psec.*[b]
Whole Cluster	37,738	−0.13%	−0.95	−5.35	−5.42
VP1	12,960	−0.46	−0.65	−5.278	−5.24
VP2	8,571	−0.42	−1.9	−5.04	−5.28
VP3	13,285	+0.27	−0.22	−7.74	−7.79
VP4	2,922	−0.34	−2.67	−12.87	−12.90

Changes in Water Accessible Surface Area for Drug-Bound Cluster

	Crystal[a]	*100 steps A.D.*[b]	*100 steps ABNR*[b]	*5 psec.*	*10 psec.*[b]
Whole Cluster	37,603	−0.11	−0.79	−4.94	−5.34
VP1	12,826	−0.46	−0.38	−5.39	−4.66
VP2	8,571	−0.48	−1.76	−4.53	−4.96
VP3	13,284	−0.32	−0.18	−2.97	−4.35
VP4	2,922	+0.40	−2.50	−13.38	−14.44

[a] Values are in Å^2

[b] Values represent percentage change from corresponding values in crystal structure used for the simulations.

clusters. However, the drug bound cluster had a smaller change in surface area for VP1, VP2 and VP3, but a larger change in VP4. The small overall decrease of about 5% in surface area indicates a relatively small distortion of the protein, and the presence of the drug appears to decrease the distortion in VP1, VP2 and VP3. In both clusters, VP4 has a much higher decrease in surface area. As VP4 has a relatively small RMS difference from the X-ray structure, this decrease could be due more to changes in its contact surfaces with the other segments than to changes in its structure.

The quality of the potential function and the simulation is reflected not only in the modest changes in the atomic positions and protein surface area, but also by the negligible changes in the radius of gyration of the clusters. For the drug free cluster, the radius of gyration changed from 31.68 Å in the crystal structure to 31.06 Å for the 10 psec dynamics average, while the corresponding values for the ligand bound complex were 31.63 Å and 31.05 Å, respectively.

The time correlation of the radius of gyration of both complexes indicated no significant periodic motions over 3 psecs of the trajectory. The radius of gyration was constant over this interval.

2. *Atomic Fluctuations of C_α atoms*

The RMS fluctuations about the dynamically averaged positions were calculated for all atoms from the 10 psec trajectories. The mean fluctuations for all atoms were 0.26 Å and 0.28 Å for the free and bound trajectories, and 0.20 Å and 0.22 Å for the C_α atoms. The mean fluctuations for all atoms of residues within 20 Å from the binding site were 0.22 Å for both trajectories and for residues within 10 Å of the binding site, the values were 0.22 Å and 0.21 Å for the free and the bound trajectories. Hence, the values for the free and bound trajectories were not significantly different from each other. In both trajectories, VP1 and VP3 had higher RMS fluctuations, due to the free amino and carboxy ends as discussed earlier. There were also no significant differences in the fluctuations of the different subunits between the two trajectories.

A scatter plot of the water accessible surface area against the fluctuation (not shown) indicates a weak correlation between the surface area and the fluctuation. Although some of the residues possessing relatively high fluctuations (between 0.2 and 0.5 Å) had very small water accessible surfaces, the majority of these residues have large surface areas. Residues with fluctuations greater than 0.5 Å usually occur in the exposed loops. A scatter plot of the distance from the center of mass geometry versus the fluctuation (not shown) indicates a weak correlation between the two variables. The residues within the RMS fluctuation range of 0.15 to 0.25 Å are distributed between 0.0 and 60 Å from the center of mass, i.e., within the bulk of the cluster. The majority of the residues with fluctuations above the mean are distributed further away, often in the external loops. The high mobility of these isolated strands was evident from movies of the trajectories on a graphics terminal.

The correlation times for the C_α carbons of every fifth amino acid residue in the complex were calculated, beginning with the fifth residue. The results indicated that the presence of the drug increased the uniformity of the correlation times τ as shown in Figures 3a–c. The average correlation time (values greater than 100 psec excluded) for the drug-free complex was 8.7 psec, (6 values excluded) with a standard deviation of 16.91, compared to an average of 4.8 psec with a standard deviation of only 11.95 psec, (2 values excluded), in the drug-bound complex. The distribution of τ is given in Table III.

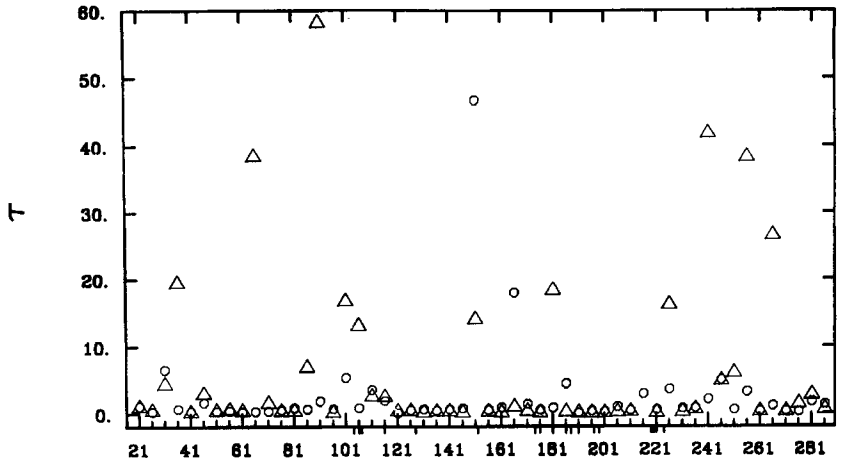

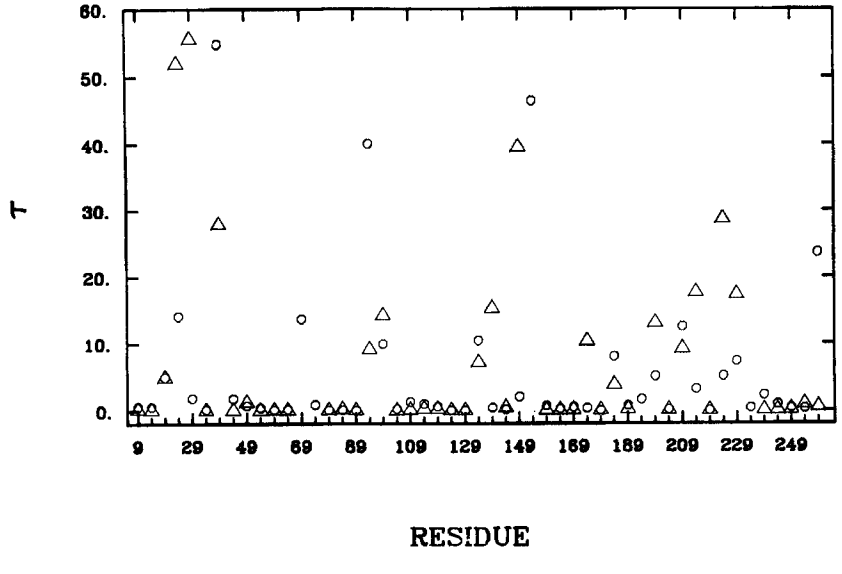

Figure 3 Plot of C_α correlation time, τ (psec) against residue number for every fifth residue out of 804 total residues. △: ligand free; ○: ligand bound. a) Plot for residues 17 to 289 of VP1. The residues in van der Waals contact are indicated by ticks below the x-axis. Only values for residues corresponding to the five residue intervals are plotted for clarity. b) Plot for residues 8 to 262 of VP2. c) Plot for residues 1 to 236 for VP3 on left and 29 to 68 for VP4 on the right.

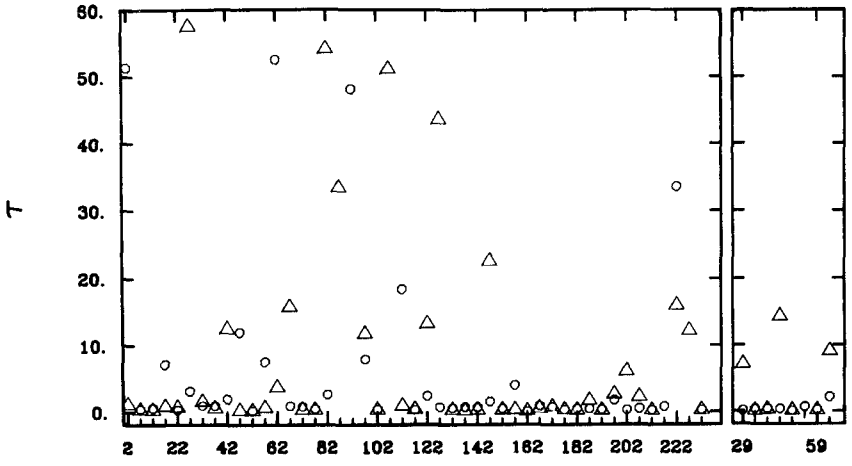

The following regions were chosen for closer examination; the FMDV loop region [res 213 to 225] and residues at the carboxyl end of the βE corner of VP1 [res 150 to 157], both of which undergo conformational changes upon binding of the drug (10), residues in the NIM1 site [residues 81 to 98]; residues between the βD and βE strands [residues 137 to 145] of VP1 and residues in the βH region of VP2 [residues 222 to 237]. The C_α correlation times of each residue in these regions were calculated. The results were similar to the overall survey of every fifth residue, i.e., a substantial decrease in extremely long correlation times, with a complementary slight increase for extremely short decay times in the presence of the drug.

An analysis of the local and collective motions in a variety of proteins (1, 22, 23) suggests that fluctuations generally involve the superposition of two types of motions. One has localized, high frequency oscillations of relatively small magnitude. The other has considerably lower frequencies and larger amplitudes; these oscillations involve the correlated motions of groups of atoms. Groups of atoms that appear to be moving together have similar correlation functions and decay times. Thus, the effect of the drug in globally reducing the inhomogeneity in the decay times suggests a corresponding decrease in the number of groups of atoms that are moving as different units. In other words, the presence of the drug appears to lead to more collective motion of the residues. This effect of the ligand appears to reach out to most of the residues, i.e.,

Table 3 Distribution of Correlation Time τ.

Correltion Time τ (psec)	*Number of Residues*	
	Without Drug	*With Drug*
< 1	91	98
$1 \leqslant \tau < 10$	25	43
$10 \leqslant \tau < 100$	38	17
$100 \leqslant \tau$	6	2

Figure 4 Plot of the normalized equal-time cross-correlation values for the position fluctuations of the C_α atoms of nineteen residues. The diagonal, representing equal-time auto-correlation values, has been zeroed out for clarity, with the exception of the value for the last residue (value of 1.0) which is left as a reference scale.

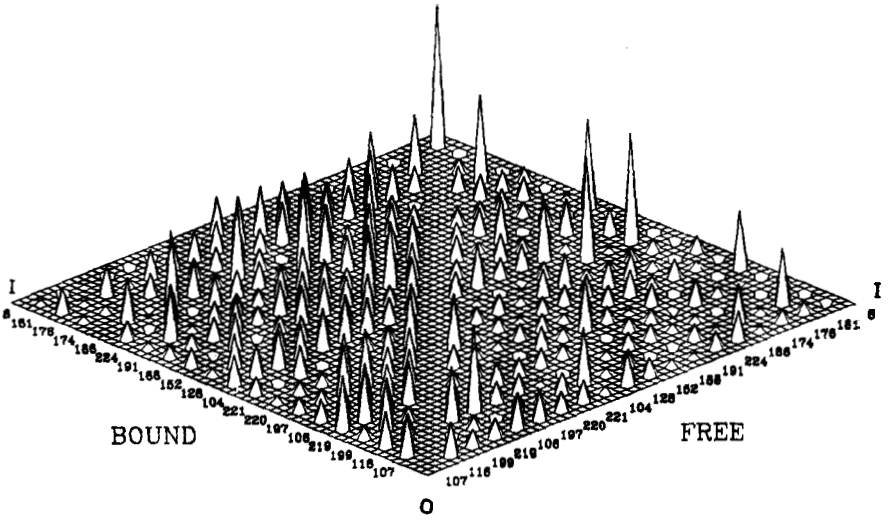

Figure 4a Values greater than zero are shown.

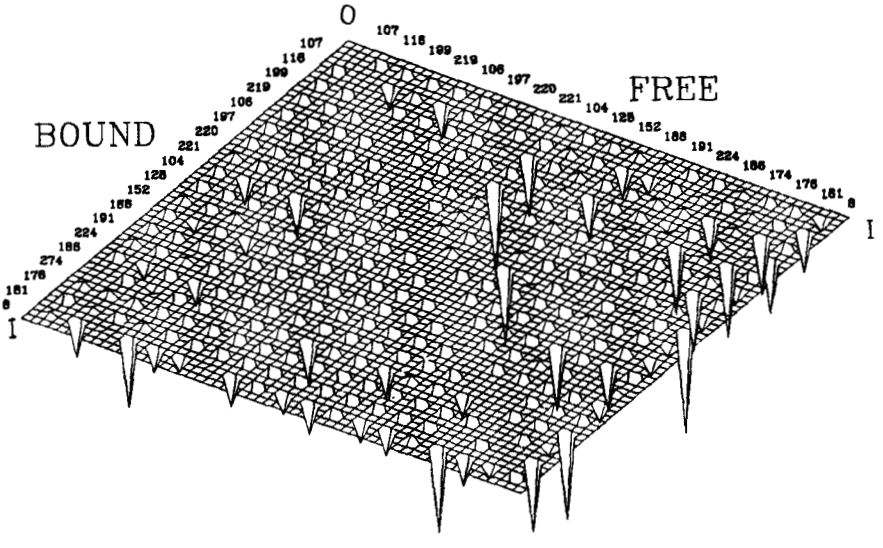

Figure 4b Rotations of the plane of Figure 4a to show values that are less than zero. The right half gives the values for the ligand-free state, while the left half gives the values for the bound state. The order of the values for residues from O to I are: first 4 in oxazole region, second 5 in phenoxy region, third 5 in aliphatic chain region and last 5 in isoxazole region.

across all of the subunits, and is not restricted to an immediate area in the vicinity of the ligand.

The cross-correlation functions for the displacement of the C_α atoms of nineteen residues were analyzed. The results are shown in the plot in Figure 4, where the left side gives the equal-time cross-correlation values for the drug-bound complex and the right side gives the values for the drug-free complex. The first seventeen residues are from VP1 and are within 3.6 Å from the drug. The eighteenth residue (from VP1) and the last residue (from VP3) are 14 Å from the isoxazole end of the drug. For the residues in VP1, the drug causes an increase in the positive correlation for the atomic fluctuations, i.e., the atoms are moving more in synchrony in comparison to those in the absence of the drug (Figure 4). In general, residues that were not correlated or that showed a negative correlation became correlated in their motion when the drug was bound, and residue pairs that had a slight positive correlation increased their correlation on binding of the drug. The few residue pairs that showed a strong positive correlation in the free state experienced a strong decrease in their correlation on binding of the drug. As seen in Figure 4, the drug decreased the cross-correlation of the motion of the residue of VP3 with the residues of VP1.

The percentage change in the RMS fluctuations about the dynamically averaged positions for these nineteen residues are given in Table IV. The first four residues are close to the oxazole region, followed by five residues in the phenoxy region, five in the aliphatic chain region, three in the isoxazole region, and two somewhat more distant from the drug. The sequence of these residues are the same as in Figure 4. There is an overall decrease in the fluctuations for residues that were in the regions of the

Table 4 RMS Fluctuations About the Dynamically Averaged Positions for Residues at the Binding Site.[a]

Residue[b]	*Interaction*[c]	*RMS Fluctuations*[d]		*%ΔF*[e,f]
		Without Drug	*With Drug*	
107	oxazole	0.13	0.15	−15.4
116	oxazole	0.39	0.20	48.7
199	oxazole	0.12	0.13	−8.3
219	oxazole	0.15	0.13	13.3
106	phenoxy	0.28	0.23	17.8
197	phenoxy	0.15	0.16	−6.7
220	phenoxy	0.19	0.15	21.1
221	phenoxy	0.28	0.23	17.9
104	phenoxy	0.55	0.47	14.5
128	aliphatic chain	0.19	0.22	−15.8
152	aliphatic chain	0.17	0.16	5.9
188	aliphatic chain	0.25	0.20	20.0
191	aliphatic chain	0.24	0.21	12.5
224	aliphatic chain	0.22	0.23	−4.5
186	isoxazole	0.33	0.27	18.2
174	isoxazole	0.17	0.21	−23.5
176	isoxazole	0.20	0.22	−10.0
181	isoxazole	0.20	0.21	−5.0
8	isoxazole	0.19	0.21	−10.5

[a] See Figure 4. Fluctuations for all atoms
[b] Residue Sequence as in Figure 4. All residues from VP1, except for the last (from VP3).
[c] Interaction of residue with functional group of drug.
[d] Fluctuations in Å.
[e] ΔF = (Fluctuations without Drug-Fluctuations with Drug).
[f] $\%\Delta F$ = (ΔF/Fluctuation without Drug) × 100.

(4-methyl-oxazolinyl)phenoxy group and the seven-membered aliphatic chain but an increase in the fluctuations in the region of the 3-methylisoxazole group. (Average decrease in fluctuations of 11 ± 6% for the seventeen residues in Van der Waals contact). The greatest change occurs in residue 116, a leucine group that is located close to the opening into the RNA interior. The fluctuations of this residue were substantially reduced by the drug.

CONCLUSIONS

Molecular dynamics simulations of the human rhinovirus coat proteins in the ligand-free state and the drug-bound state have been analyzed. The proteins remained stable during the period of the data collection, as evidenced by the minor changes in structure (i.e., changes in atomic positions, radius of gyration and surface area).

The presence of the drug did not cause any significant changes in the RMS fluctuations of the residues or C_α atoms far from the binding site. Although it did not significantly affect the high frequency oscillations, it affected the lower frequency oscillations which involve the correlated motions of groups of atoms. The ligand reduced the inhomogeneity in the C_α decay times, which is indicative of a more collective motion of the residues. This effect appeared to be distributed throughout the cluster (excluding the loose terminal strands) as seen from the results in Figure 3. This could be due to the intricate contacts between the different subunits as discussed above, which propagate the effect of the drug throughout the complex. The atoms in the immediate vicinity of the binding site moved with smaller amplitudes, collectively, and in phase in the presence of the drug.

These results can be qualitatively interpreted in terms of a simple mechanical model. The residues can be thought of as independent, equivalent one-dimensional overdamped harmonic oscillators that become linked by the drug molecule. If two such oscillators are so linked, the RMS amplitudes of each will decrease by about 30%, the correlation time will decrease by about 50%, and the normalized cross-correlation of positional fluctuations will increase from zero to one. Similar effects are observed for most of the residues adjacent to the drug binding site, and the results in Fig. 3 suggest that the rigidification of the binding site has an influence on the dynamics of the whole protein cluster. It has been suggested, from experiments, that the binding of the des-methyl analog, WIN 51711 (Figure 2) (10), to the coat protein stabilizes the protein coat (24).

It should be mentioned that as the holoprotein structure was used to simulate both the apo and the holo systems, the differences in the dynamical behavior observed here may be thought to be artificial. As mentioned earlier, the apoprotein differs structurally in the chain leading from the FMDV loop of VP1 and at the carboxyl end of the *β-E* corner of VP1. The dynamics of the apoprotein observed here might represent the initial relaxation of this holoprotein structure to the apostructure. Hence, we have simulated the actual apoprotein structure following the same minimization, heating, and equilibration used for the runs discussed in detail herein. The preliminary indications of this simulation, which will be reported in full in a later paper together with the results of a simulation of the ligand-protein complex in aqueous surroundings, also confirm the central finding in this work of the ligand induced reduction of the inhomogeneity of relaxation times in the coat proteins.

Acknowledgements

We thank Prof. J.A. McCammon for many interesting and useful discussions as well as his thoughts on the oscillator analogy. We would like to thank Professor Michael Rossmann and his group at Purdue University for providing us with x-ray coordinates for the drug-virus complexes. We would also like to thank the Sterling-Winthrop Research Institute for experimental data for the compounds examined in this study. This work was supported in part by grants from the Robert A. Welch Foundation, the Texas Advanced Technology Research Program, The Tektronix Corporation, and The Sterling-Winthrop Research Institute. TPL was the recipient of a Damon Runyon-Walter Winchell Cancer Fund Fellowship Award, DRG-888. WFL and TPL were also supported in part by grants to J.A. McCammon from the NSF and the R.A. Welch Foundation. Some of the analysis was made possible by a grant of time from the San Diego supercomputer center.

References

[1] J.A. McCammon, S.C. Harvey, *Dynamics of proteins and nucleic acids*. Cambridge University Press, Cambridge, 1987.

[2] J.A. McCammon, B.R. Gelin, M. Karplus, "Dynamics of Folded Proteins". *Nature (London)* **267**, 585–590, (1977).

[3] M. Prabhakaran, J.A. McCammon, S.C. Harvey, "Atomic Motions in Phenyl Alanine Transfer RNA Probed by Molecular Dynamics Simulations", *Mol. Basis of Cancer, Part A: Macromolecular Structure, Carcinogens, and Oncogenes*. 123–129, (1985).

[4] S.H. Northrup, M.R. Pear, J.D. Morgan, J.A. McCammon, "Molecular Dynamics of Ferrocytochrome C", *J. Mol. Biol* **153**, 1087–1109, (1981).

[5] P. Kruger, W. Stassburger, A. Wollmer, W.F. van Gunsteren, "A Comparison of the Structure and Dynamics of Avian Pancreatic Polypeptide Hormone in Solution and in the Crystal". *Europ. Biophy. J.*, **13**, 77–88, (1985).

[6] C.F. Wong, J.A. McCammon, "Dynamics and Design of Enzymes and Inhibitors", *J. Amer. Chem. Soc.*, **108**, 3830–3832, (1986).

[7] P. Ahlstrom, O. Teleman, B. Jonsson, S. Forsen, "Molecular Dynamics Simulation of Parvalbumin in Aqueous Solution", *J. Amer. Chem. Soc.*, **109**, 1541–1551, (1987).

[8] A.T. Brunger, C.L. Brooks III, M. Karplus, "Active Site Dynamics of Ribonuclease", *Proc. Natl. Acad. Sci. USA* **82**, 8458–8462, (1985).

[9] C.B. Post, B.R. Brooks, M. Karplus, C. Dobson, P. Artymiuk, J.C. Cheetham, D.C. Philips, "Molecular Dynamics Simulations of Native and Substrate Bound Lysozyme" *J. Mol. Biol.* **190**, 455–479, (1986).

[10] T.J. Smith, M.J. Kremer, M. Luo, G. Vriend, E. Arnold, G. Kamer, M.G. Rossman, M.G. McKinlay, G.D. Diana, M.J. Otto, "The site of Attachment in Human Rhinovirus 14 for Antiviral Agents that inhibit Uncoating", *Science* **233**, 1286–1293, (1986).

[11] R.R. Rueckert, "On the Structure and Morphogenesis of Picornaviruses", in *Comprehensive Virology*, H. Fraenkel-Conrat and R.R. Wagner, Eds.(Plenum, New York, 1976) vol. 6. pp. 131–213.

[12] J.A. McCammon, "Computer Aided Molecular Design", *Science* **238**: 486–491, (1987).

[13] T.P. Lybrand, W.F. Lau, J.A. McCammon, B.M. Pettitt, "Molecular Dynamics Studies of Antiviral Agents: Thermodynamics of Solvation and Binding", in *Protein Structure and Design*, UCLA Symposia on Molecular and Cellular Biology, New Series, Vol. 69, D. Oxender, Ed. (Alan R. Liss, New York, 1987) pp. 227–233.

[14] G.D. Diana, M.A. McKinlay, M.J. Otto, V. Akullian, C. Oglesby, "[[(4,5-Dihydro-2-oxazoly)phenoxy]alkyl]isoxazoles. Inhibitors of Uncoating", *J. Med. Chem.* **28**, 1906–1910, (1985).

[15] B.R. Brooks, R.E. Bruccoleri, B.D. Olafson, D.J. States, S. Swaminathan, M. Karplus, "CHARMM: A Program for macrmolecular Energy, Minimization and Dynamics Calculations", *J. Comput. Chem.* **4**, 187–217, (1983).

[16] L. Verlet, "Computer Experiments on Classical Fluids. I: Thermodynamical Properties of Lennard-Jones Molecules", *Phys. Rev.*, **159**, 98–103, (1967).

[17] W.F. van Gunsteren, H.J.C. Berendsen, "Algorithms for Macromolecular Dynamics and Constrained Dynamics", *Mol. Phys.* **34**, 1311–1327, (1977).

[18] M.G. Rossman, E. Arnold, J.W. Erickson, E.A. Frankenberger, J.P. Griffith, H.J. Hecht, J.E. Johnson, G. Kamer, G.M. Luo, A.G. Mosser, R.R. Rueckert, B. Sherry, G. Vriend, "Structure of a Human Common Cold Virus and Functional Relationships to Other picornaviruses", *Nature (London)* **317**, 145–153 (1985).

[19] M. Levitt, "Molecular Dynamics of Native Proteins II. Analysis and Nature of Motion", *J. Mol. Biol.***168**, 595–620, (1983).

[20] S.H. Northrup, M.R. Pear, J.A. McCammon, M. Karplus, T. Takano, "Internal Mobility of Ferrocytochrome C", *Nature (London)* **287**, 659–660, (1980).

[21] F.M. Richards, "Areas, Volumes, Packing and Protein Structure", Annu. *Rev. of Biophys. Bioeng.* **6**, 151–176 (1977).

[22] M. Karplus, S. Swaminathan, T. Ichiye, W.F. van Gunsteren, "Local and Collective Motions in Protein Dynamics", in *CIBA Foundation Syposium 93. Mobility and Functions in Proteins and Nucleic Acids* (Pitman, London, 1983) pp. 271–290.

[23] C.L. Brooks, M. Karplus, B.M. Pettitt, "Proteins: A Theoretical Perspective of Structure Dynamics and Thermodynamics", *Adv. in Chem. Phys.* (1988) in press.

[24] M.P. Fox, M.J. Otto, M.A. McKinlay, "The Prevention of Rhinovirus and Poliovirus Uncoating by WIN51711: A New Antiviral Drug", *Antimicrob. Agents Chemother.* **30(1)**, 110–116, (1986).